The Opioid Growth Factor (OGF)–OGF Receptor Axis Uses the p16 Pathway to Inhibit Head and Neck Cancer

Fan Cheng,[1] Ian S. Zagon,[1] Michael F. Verderame,[2] and Patricia J. McLaughlin[1]

Departments of [1]Neural and Behavioral Sciences and [2]Medicine, The Pennsylvania State University College of Medicine, Hershey, Pennsylvania

Abstract

Head and neck squamous cell carcinoma (HNSCC) represents 5.5% of malignancies worldwide, with ~30,000 new cases and ~11,000 deaths reported in the United States annually. The opioid growth factor (OGF; [Met^5]-enkephalin) and the OGF receptor (OGFr) form an endogenous growth regulating system; the OGF-OGFr axis influences the G_0-G_1 phase of the cell cycle in HNSCC. Cells treated with small interfering RNA (siRNA) for OGFr no longer responded to the growth inhibitory effects of OGF or the growth stimulatory effects of naltrexone, indicating that these activities are entirely mediated by OGFr. In this investigation, we examined the precise target of OGF in the cell cycle. Using SCC-1 cells, OGF decreased the phosphorylation of retinoblastoma protein. This change was correlated with reduced Cdk4, but not Cdk2, kinase activity. OGF treatment increased cyclin-dependent kinase inhibitor p16 protein expression. Importantly, p16 complexed with Cdk4 was increased by OGF treatment at all time points, consistent with the hypothesis that OGF mediated growth inhibition through p16. Blockade of OGF-OGFr interactions with naloxone abolished the increased expression of p16 protein by OGF. Inhibition of p16 (INK4a) activation by p16-specific siRNA blocked OGF's repressive action on proliferation of SCC-1, CAL-27, and SCC-4 HNSCC cells. These data are the first to reveal that the target of cell proliferative inhibitory action of OGF in human HNSCC is a cyclin-dependent kinase inhibitory pathway, and this may be useful in the diagnosis and treatment of HNSCC. [Cancer Res 2007;67(21):10511–8]

Introduction

The opioid growth factor (OGF), chemically termed [Met^5]-enkephalin, is an endogenous opioid peptide that is an important regulator of the progression of human head and neck squamous cell carcinoma (HNSCC; refs. 1–3). OGF is a constitutively expressed native opioid that is autocrine produced and secreted and interacts with the OGF receptor (OGFr) to inhibit the growth of HNSCC cells *in vitro* and in tumor xenografts (2–4). The action of OGF is tonic, stereospecific, reversible, noncytotoxic, and nonapoptotic-inducing, not associated with differentiative, migratory, invasive, or adhesive processes, independent of serum, anchorage-independent, and occurs at physiologically relevant concentrations in a wide variety of HNSCC cancers, including poorly and well-differentiated human cell lines (1, 3, 4). The only opioid peptide, natural or synthetic, that influences the growth of HNSCC is OGF (4). The action of this opioid in these neoplasias is targeted to DNA synthesis (5) and is directed toward the G_0-G_1 interface of the cell cycle (6). Exogenous administration of OGF has a profound antitumor action on xenografts of HNSCC that includes delaying tumor appearance and reducing tumor size (1, 2). The combination of biotherapy with OGF and chemotherapy with paclitaxel has proved to enhance antitumor effectiveness beyond either agent alone (2, 3).

The gene for human OGFr is at least 9 kb in length, composed of seven exons and six introns, and encodes a 677–amino acid protein that includes seven imperfect repeats of 20 amino acids each and a bipartite nuclear localization signal (7). OGFr has an apparent mass of 62 kDa. The chromosomal location of the human OGFr is 20q13.3 (7). Although OGFr has characteristics of a classic opioid receptor (recognizes opioids, naloxone reversibility, stereospecificity), there is no homology of OGFr with classic opioid receptors in terms of nucleotides or amino acids (7). Antisense experiments with OGFr and continuous blockade of opioid receptors by the potent opioid antagonist naltrexone support that the OGF-OGFr axis is a tonically active inhibitory system targeted to cell replication and homeostasis and is ligand-dependent for function (7). Immunoelectron and confocal microscopy have shown that OGFr is localized to the outer nuclear envelope, nucleus, and perinuclear cytoplasm (8, 9). Gene expression (7) and protein expression (7) of OGFr, as well as binding activity (7), have been identified and characterized in HNSCC cell lines, revealing the autocrine nature of this growth regulatory axis.

Given that OGF is known to influence cell proliferation and that flow cytometry studies indicate that the G_0-G_1 of the cell cycle is altered, the present investigation examined the specific target(s) with the cell cycle for the OGF-OGFr axis.

Materials and Methods

Cell culture. The SCC-1 cell line was obtained from the University of Michigan Cancer Research Laboratory (Thomas E. Carey, Ph.D.), and CAL-27 and SCC-4 cells were obtained from the American Type Culture Collection. SCC-1 and CAL-27 cells were cultured in DMEM media, whereas SCC-4 cells were grown in 1:1 Hams F-12 DMEM media. All media (Penn State University) was supplemented with 10% fetal bovine serum (HyClone), 1.2% sodium bicarbonate, and 5,000 units/mL penicillin, 5 μg/mL streptomycin, and 10 μg/mL neomycin.

OGF treatment. OGF was purchased from Sigma-Aldrich, dissolved in sterile water, and used at a final concentration of 10^{-6} mol/L.

Cell growth and flow cytometry. For growth curves, cells were seeded in six-well plates at an initial density of $\sim 2 \times 10^5$ cells per well. Fresh media and OGF were added 24 h after initial seeding, and media and OGF were replaced daily. At appropriate times, the cells were washed with PBS and trypsinized, and viable cell numbers were counted by trypan blue exclusion using a hemacytometer.

For flow cytometry, cells were synchronized with 0.5 μg/mL nocodazole (Sigma-Aldrich) for 24 h, followed by three washes with complete media. Cells were released from growth arrest by addition of complete media or

Requests for reprints: Patricia J. McLaughlin, Department of Neural and Behavioral Sciences, H109, The Milton S. Hershey Medical Center, 500 University Drive, Room C3727, Hershey, PA 17033. Phone: 717-531-6414; Fax: 717-531-5003; E-mail: pxm9@psu.edu.

doi:10.1158/0008-5472.CAN-07-1922

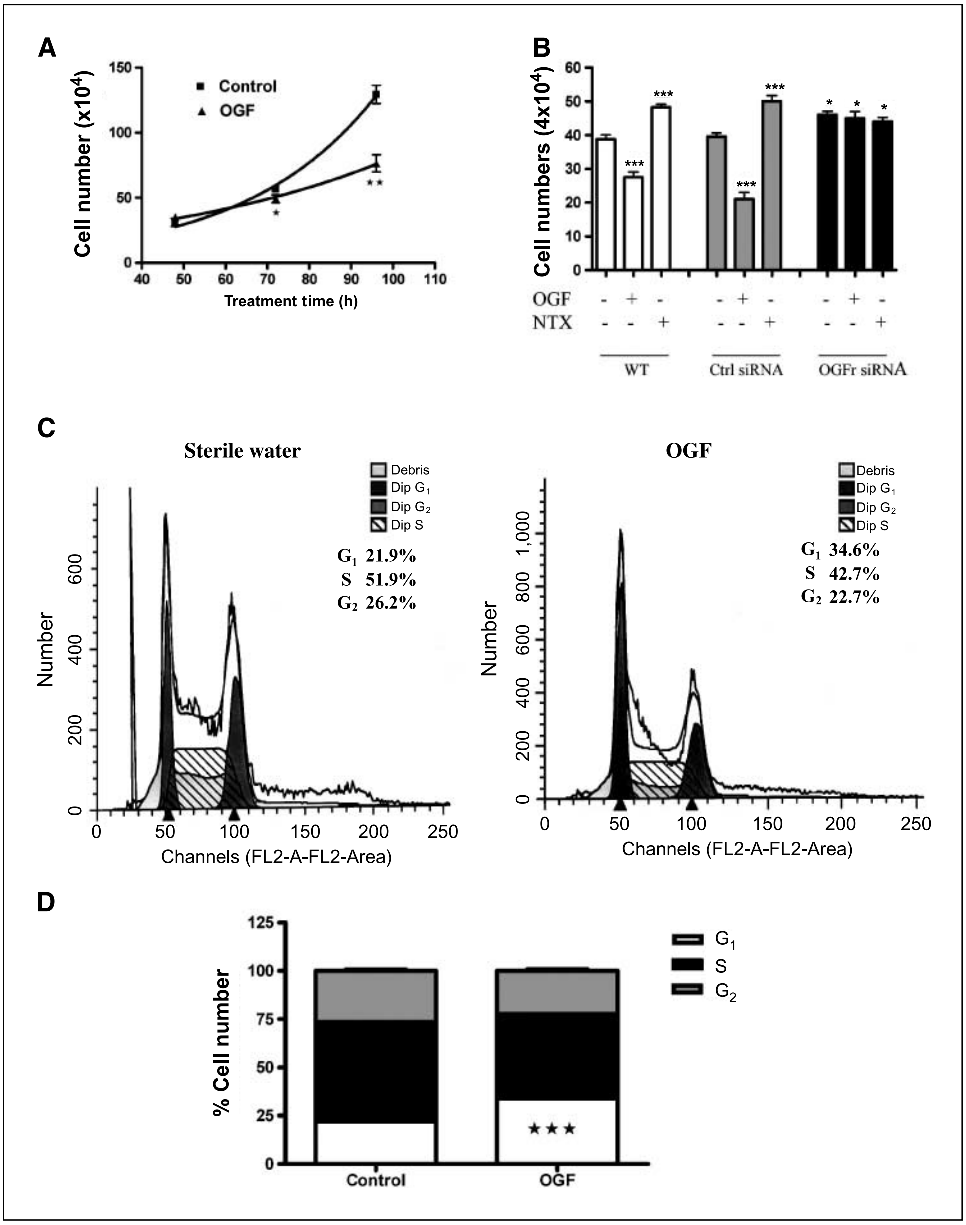

Figure 1. OGF inhibits SCC-1 growth by arresting cells in G_1. *A,* SCC-1 cells were grown in the presence of 10^{-6} mol/L OGF for 96 h. Cells were counted after 48, 72, or 96 h of treatment. The number of cells in OGF-treated cultures were significantly reduced from control cultures receiving sterile water at 72 h (★, $P < 0.05$) and 96 h (★★, $P < 0.01$). *B,* OGFr is required for OGF action on growth. SCC-1 cells were transfected with OGFr siRNAs or control siRNAs for 24 h in the presence of 10^{-6} mol/L OGF, 10^{-6} mol/L naltrexone (*NTX*), or sterile water. Cells were harvested at 96 h and counted with a hemacytometer. *Columns,* means for two independent experiments; *bars,* SE. Cell numbers differed from wild-type (*WT*) or control (*Ctrl*) siRNA treated with sterile water at $P < 0.001$ (★★★). Cell numbers differed from wild-type cultures treated with sterile water at $P < 0.05$ (★). *C,* flow cytometry of synchronized SCC-1 cells subjected to sterile water (control) or OGF for 14 h as determined by fluorescence-activated cell sorting analysis. *D,* percentage of cells in G_1, S, and G_2 phases. Data represent means of three experiments. The percentage of OGF-treated cells in G_1 was significantly elevated from control values at $P < 0.001$ (★★★).

OGF-supplemented media. Synchronized cells were treated with 10^{-6} mol/L OGF for 14 h, harvested with 0.25% trypsin-EDTA (Mediatech), and fixed with 70% ethanol at $-20°C$ for up to 7 days before DNA analysis. DNA content was obtained by incubating cells in PBS containing propidium iodide (0.1 mg/mL) and RNase A (0.02 mg/mL) for 15 min at 22°C. Fluorescence was measured and analyzed using a BD Biosciences FACScan flow cytometer and Modfit Software.

Small interfering RNA knockdown of OGFr. The OGFr-targeted small interfering RNAs (siRNA; antisense, 5′-uagaaacucagguuuggcg-3′; sense, 5′-cgccaaaccugaguuucua-3′) were designed and obtained as ready-annealed, purified duplex probes from Ambion. For transfection, 5×10^4 cells per well were seeded in six-well plates containing 1 mL of serum-containing media without antibiotics. In each well, 20 nmol/L OGFr-siRNA or control siRNAsolutions in serum-free media were added. Cells were incubated for 4 h at 37°C before the addition of OGF. Cultures were incubated for an additional 20 h, and then 1-mL fresh complete media, either lacking or containing OGF, was added. At 96 h, cells were collected for computing growth. Two independent experiments were conducted. The control siRNAs were purchased from Ambion.

Western blot analysis. Synchronized cells ($\sim 2 \times 10^6$) from each treatment were solubilized in 200 μL radioimmunoprecipitation assay buffer (1× PBS, 10 μmol/L IGEPAL, 1 mg/mL SDS, 5 mg/mL deoxycholic acid), containing protease and phosphatase inhibitors [2 μg/mL aprotinin, 3 mg/mL phenylmethylsulfonyl fluoride (PMSF), 1 mmol/L sodium orthovanidate, 1 μmol/L okadaic acid]. Total protein concentrations were measured using the detergent-compatible protein assay kit (Bio-Rad Laboratories). Equal amounts of protein (40 μg) were subjected to 10% SDS-PAGE, followed by transfer of proteins onto polyvinylidene difluoride (Millipore) using standard protocols. The following antibodies were purchased from commercial sources: phosphorylated retinoblastoma ($Ser^{807/811}$) from Cell Signaling Technology; phosphorylated retinoblastoma (Thr^{821}) from Biosource,; Cdk4, cyclin D1, p15, p16, p18, and p19 from Santa Cruz Biotechnology; total retinoblastoma, p21, and p27 from BD PharMingen; and β-actin (Clone AC-15) from Sigma. The following dilutions of primary antibodies were used to detect respective proteins: 1:200 phosphorylated retinoblastoma ($Ser^{807/811}$), 1:200 phosphorylated retinoblastoma (Thr^{821}), 1:200 Cdk4, 1:200 cyclin D1, 1:100 p16, 1:200 total retinoblastoma, 1:200 p21, 1:100 p27. Membranes were probed with secondary antirabbit or antimouse horseradish peroxidase–conjugated antibodies (GE Healthcare-Amersham Biosciences); blots were developed using a chemiluminescence Western blotting detection system (GE Healthcare-Amersham Biosciences).

To determine equal loading of total protein samples, blots were reprobed with monoclonal antibody against β-actin at a dilution of 1:2,000. If necessary, membranes were stripped in stripping buffer [62.5 mmol/L Tris-HCl and 100 mmol/L β-mercaptoethanol/2% SDS (pH 6.7)] at 50°C before being reprobed. Means and SE were determined from three or more independent experiments.

Quantitation of Western blots. To quantify expression levels or kinase activity, the absorbance of each band was determined by densitometry and analyzed by QuickOne (Bio-Rad Laboratories). Each value was normalized to β-actin from the same blot. To report the changes due to OGF treatment, we calculated the fold increase by dividing the normalized value from the OGF-treated samples by the normalized value of control samples at each time point; thus, increases due to OGF have values of >1 and decreases due to OGF have values of <1.

Immunoprecipitation and retinoblastoma kinase assay. For immunoprecipitating protein complexes, cell extracts were prepared as follows: 2×10^6 cells per sample were rinsed in cold PBS, followed by lysis in 100 μL NP40 immunoprecipitation buffer [1% NP40, 50 mmol/L Tris-HCl (pH 7.4), 150 mmol/L NaCl, 1 mmol/L EDTA, 10 mmol/L NaF, 2 μg/mL antipain, 1 mmol/L sodium orthovanidate, 2 μg/mL aprotinin, 2 μg/mL leupeptin, 1 μg/mL pepstatin A, 1 μmol/L okadaic acid, 1 mmol/L PMSF, 1 mmol/L DTT]. For each immunoprecipitation reaction mixture, a total of 500 μg of protein extract was used. The lysates were then subjected to immunoprecipitation using 10 μL polyclonal antibody against Cdk4 prebound with agarose conjugate (Santa Cruz) for 60 min at 4°C. Then immunoprecipitates were mixed with kinase buffer [25 mmol/L HEPES (pH 7.4), 10 mmol/L $MgCl_2$], 5 μCi γ^{32}P-ATP, and retinoblastoma (769–921; Santa Cruz) as the substrate for Cdk4. After incubation for 30 min at 30°C, with occasional mixing, the reaction was stopped by the addition of 2× sample loading buffer [0.5 mol/L Tris-HCl (pH 6.8), 4.4% (w/v) SDS, 20% (v/v) glycerol, 2% (v/v) 2-mercaptoethanol, and bromophenol blue in distilled/deionized water]. Proteins in the reaction mixture were separated by a 10% SDS-PAGE gel. The Cdk4 kinase activity pattern was visualized by autoradiography of phosphorylated retinoblastoma.

p16/Cdk4 assay. Cell extracts were subjected to immunoprecipitation using antibodies against Cdk4 and protein A beads (Santa Cruz). Immunoprecipitates were separated on a 15% SDS-PAGE gel and membrane blots probed with p16 antibodies (1:200) and developed using a chemiluminescence Western blotting detection system as described earlier. Blots were reprobed with Cdk4 antibody (1:200). Five independent experiments were done.

siRNA knockdown of p16^{INK4a}. The p16-targeted siRNAs (antisense, 5′-acaccgcttctgccttttctt-3′; sense, 5′-gaaaaggcagaagcggtgttt-3′; ref. 10) were obtained as ready-annealed, purified duplex probes (Invitrogen). For

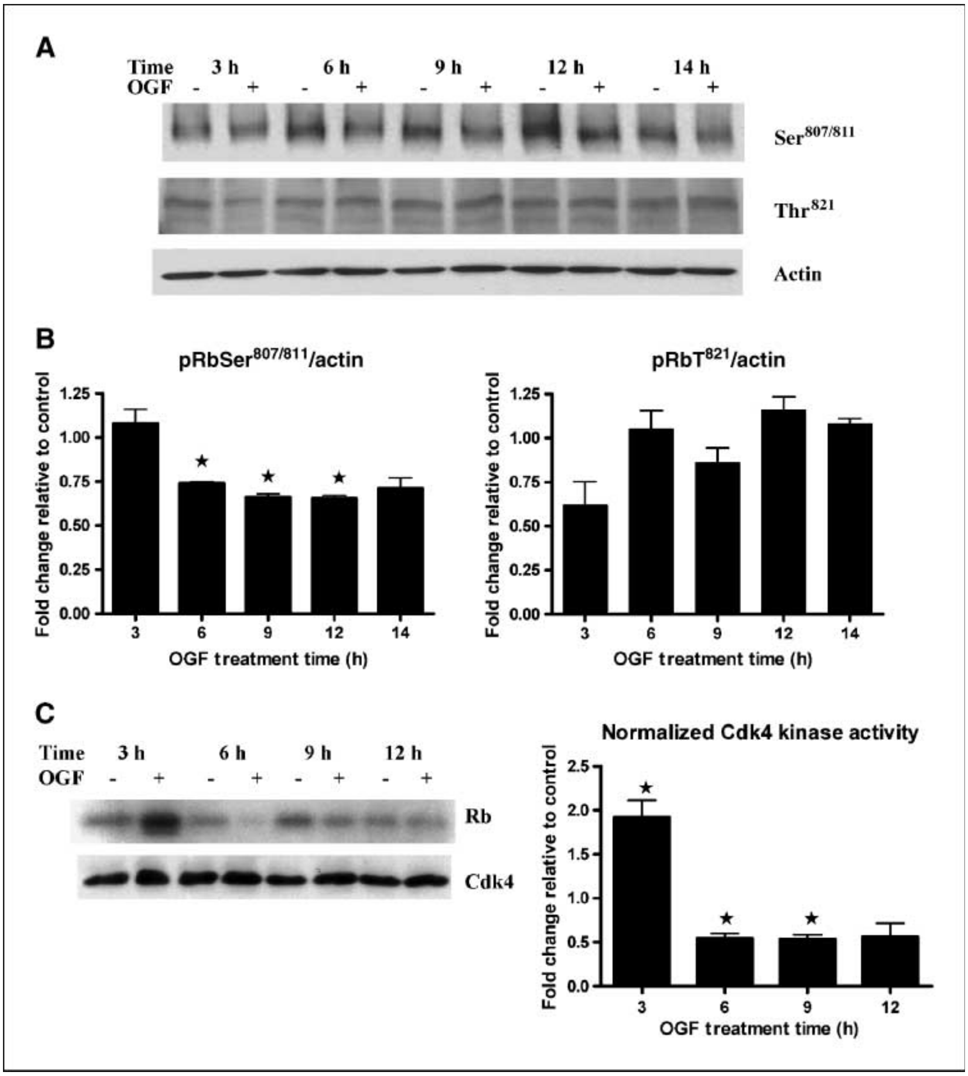

Figure 2. Inhibition of retinoblastoma (*Rb*) phosphorylation and Cdk4 kinase activity by OGF. *A,* synchronized cells were grown in the presence of OGF and harvested at 3, 6, 9, 12, and 14 h. Equal amounts of protein were analyzed by Western blot using specific antibodies recognizing phosphorylated retinoblastoma (Ser$^{807/811}$) or retinoblastoma (Thr^{821}) and normalized to actin. *B,* densitometric analysis of Western blots in (*A*). OGF-induced retinoblastoma phosphorylation is expressed relative to controls and was significantly (★, $P < 0.05$) reduced from respective controls at 6, 9, and 12 h. No changes in total retinoblastoma were noted. *C,* Cdk4 kinase activity was evaluated in synchronized SCC-1 cells treated with OGF for 3, 6, 9, or 12 h. Cdk4 kinase activity was measured as the capacity of phosphorylation of retinoblastoma protein in the presence of radioactive ATP. Densitometric analysis of the Western blots was done, and the Cdk4 activity was measured relative to controls. *Columns,* means for three independent experiments; *bars,* SE. Kinase activity values from OGF-treated cultures differed significantly (★, $P < 0.05$) from control cells at each respective time.

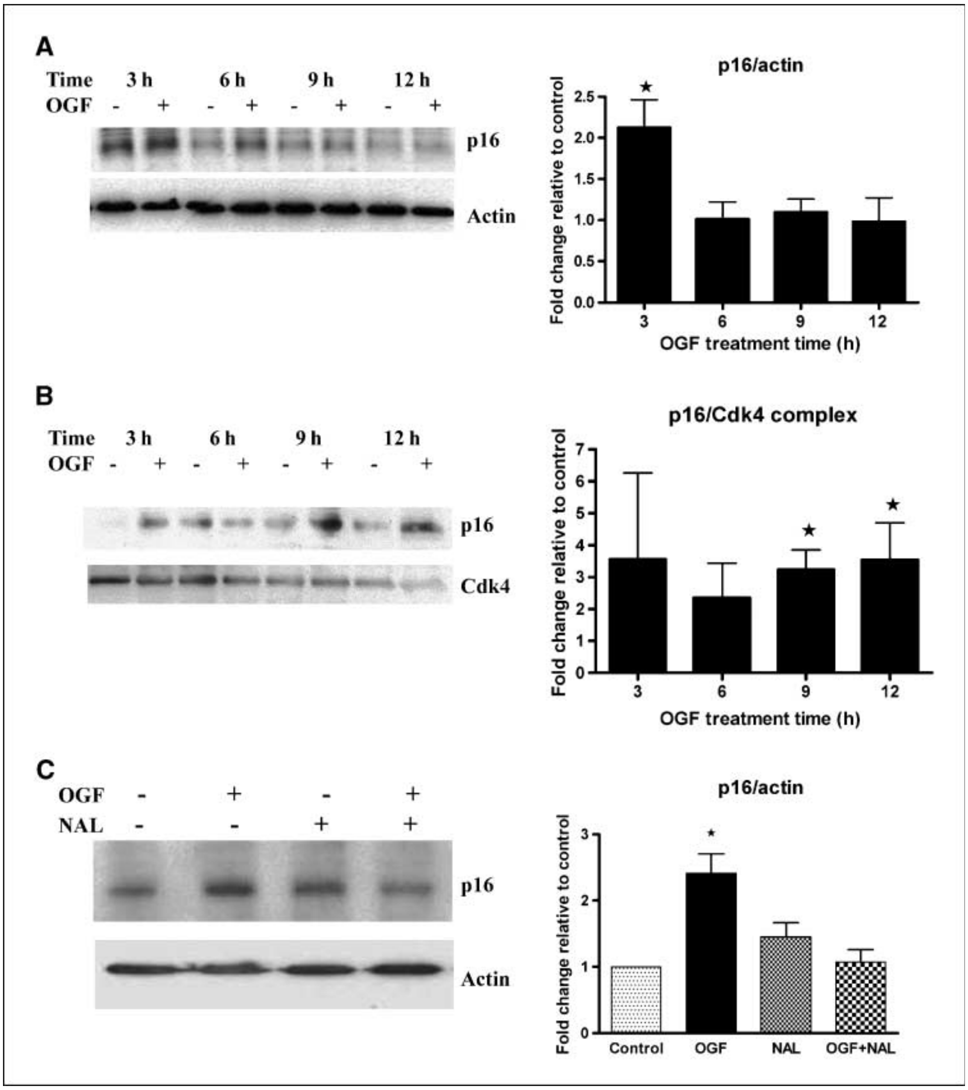

Figure 3. OGF-induced p16 expression. *A,* SCC-1 cells were synchronized by nocodazole (0.5 μg/mL) for 24 h and subsequently treated with 10^{-6} mol/L OGF or sterile water for 3, 6, 9, and 12 h. Total proteins were resolved by SDS-PAGE and blotted with p16-specific antibodies. Densitometric analysis of the Western blots was done, and p16 expression for OGF-treated cells is expressed relative to controls at each time point. The p16 level was significantly elevated (★, $P < 0.05$) from the control group at 3 h. *B,* to examine whether the OGF-induced down-regulation of Cdk4 kinase activity was based on p16-Cdk4 complex formation, homogenates of SCC-1 cells treated with OGF or sterile water were subjected to Cdk4 immunoprecipitation; the resulting proteins were blotted with antibodies to p16. Densitometric analysis of Western blots of immunoprecipitated p16-Cdk4 protein complex at 3, 6, 9, and 12 h revealed that p16 complexed to Cdk4 was increased at all time points and was significantly different from control group at $P < 0.05$ (★) at 9 and 12 h. *C,* to examine for opioid receptor mediation, synchronized cells were treated with 10^{-6} mol/L OGF, 10^{-5} mol/L naloxone (*NAL*), both OGF and naloxone, or sterile vehicle (control) for 3 h. Protein lysates were resolved on SDS-PAGE and subjected to Western blot analysis for p16 and actin. Densitometric analysis of p16 expression showed that p16 levels of OGF-treated cells were significantly elevated from control levels at $P < 0.05$ (★); no change was recorded in the naloxone and OGF-naloxone groups. *Columns,* means for three independent experiments; *bars,* SE.

transfection, 2×10^5 cells per well were seeded in six-well plates containing 1 mL of serum-free media without antibiotics. In each well, 20 nmol/L of p16-siRNA or control siRNAsolutions in serum-free media were added. Cells were incubated for 4 h at 37°C before the addition of OGF. Cultures were incubated for additional 20 h, and then 1 mL fresh complete media, either lacking or containing OGF, was added. At the indicated time points, cells were collected for growth curves or Western blotting. Three or more independent experiments were conducted. The control siRNAs were purchased from Ambion.

Statistical analysis. Values were assessed by one-way ANOVA and Newman Keul's post–multiple comparison tests. Differences were considered statistically significant at $P < 0.05$.

Results

OGF inhibits cell proliferation and retards progression through the cell cycle. Continuous exposure to exogenous OGF inhibited the growth of SCC-1 human HNSCC cells. Cell number in the OGF-treated wells was 87.5% compared with controls at 72 h and 59.0% of controls at 96 h (Fig. 1*A*). Linear regression analysis of the data revealed mean doubling times for the OGF and control groups of ∼41.3 and 21.6 h, respectively, and differed from each other at $P < 0.001$.

To examine the specificity of OGF for OGFr, knockdown experiments with OGFr-siRNA were conducted (Fig. 1*B*). Exposure to 10^{-6} mol/L OGF depressed the growth of wild-type and control siRNA-treated cells by 29% and 46%, respectively, whereas 10^{-6} mol/L naltrexone increased the number of wild-type and control siRNA-exposed cells by 24% and 27%, respectively. SCC-1 cells subjected to OGFr-siRNA had ∼19% more cells than wild-type and control siRNA-treated cultures. In contrast to cells expressing OGFr, exposure to 10^{-6} mol/L OGF or naltrexone had no further effects on the OGFr-siRNA cultures.

Based on growth curves, we analyzed the effect of OGF on cell cycle distribution by flow cytometry (Fig. 1*C*). The percentage of OGF-treated cells in the G_0-G_1 phase was 34.6% compared with 21.9% of the control cells (Fig. 1*D*); this increase in the number of cells in the G_0-G_1 phase was significantly ($P < 0.001$) different from sterile water control values. Correspondingly, the number of OGF-exposed cells in the S phase decreased to 42.7% relative to 51.9% of the sterile water–treated cells. The number of cells subjected to OGF in the G_2-M phase was 22.7% relative to 26.2% for control samples.

OGF treatment does not change total retinoblastoma protein but decreases the amount of phosphorylated retinoblastoma. The phosphorylation of retinoblastoma protein is necessary for cells to progress from G_1 phase to S phase. To elucidate the role of retinoblastoma in OGF-induced SCC-1 cell growth inhibition, retinoblastoma expression and the phosphorylated state of retinoblastoma were assessed in synchronized SCC-1 cells. Expression of total retinoblastoma protein was not decreased from baseline values after 14 h of OGF treatment (data not shown). However, the level of phosphorylated retinoblastoma ($Ser^{801/811}$), which is specifically phosphorylated by Cdk4 in the G_1 phase (11), was significantly decreased after a 6-h, 9-h, and 12-h exposure to 10^{-6} mol/L OGF (Fig. 2*A and B*). Although phosphorylated retinoblastoma ($pThr^{821}$) was specifically phosphorylated by Cdk2 in the G_1 phase (11), OGF treatment did not alter the results of Western blot analysis of phosphorylated retinoblastoma ($pThr^{821}$) levels (Fig. 2*A and B*). These results suggest that Cdk4, but not Cdk2, was involved in the OGF-induced cell cycle block at the G_1 phase in SCC-1 cells.

Total levels of p105 and p107, which are alternative pathways to retinoblastoma regulation, revealed no changes in basal levels of proteins after exposure to OGF (data not shown).

OGF reduces Cdk4 kinase activity. To verify whether OGF-induced down-regulation of phosphorylated retinoblastoma was associated with changes in Cdk4, Cdk4 expression, and activity levels were determined. The expression of Cdk4 protein did not change after OGF exposure (Fig. 2*C*). When retinoblastoma was used as substrate in immunoprecipitation experiments done with antibodies against Cdk4, lysates from cells treated with OGF for 3 h showed a transient increase of Cdk4 kinase activity; at 6, 9, and 12 h, there was a marked decrease in Cdk4 kinase activities relative to controls (Fig. 2*C*). These results suggest that OGF-mediated decrease of phosphorylated retinoblastoma was correlated with the reduction in Cdk4 kinase activities.

OGF does not affect the cyclin D-Cdk4 complex. To examine whether the OGF-induced down-regulation of Cdk4 kinase activity was based on a decrease in cyclin D1 expression, homogenates of SCC-1 cells were subjected to Cdk4 immunoprecipitation. Cyclin D1 protein levels were assessed by Western blotting. The level of the cyclin D1-Cdk4 complex after treatment with OGF revealed no change from control levels (data not shown).

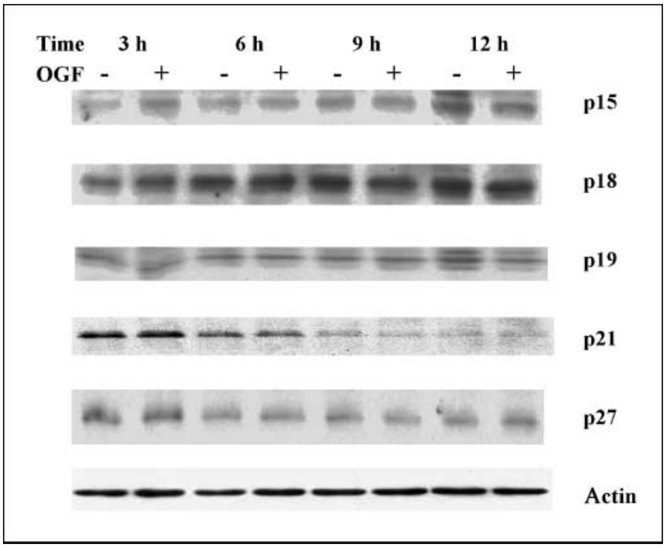

Figure 4. OGF has no effect on CKIs p15, p18, p19, p21, and p27 expression. SCC-1 cells were synchronized by nocodazole (0.5 μg/mL) for 24 h and subsequently treated with 10^{-6} mol/L OGF for 3, 6, 9, or 12 h. Total protein lysates were resolved by SDS-PAGE and subjected to antibodies specific to each CKI. Densitometic analysis revealed no significant differences between OGF and sterile water–treated values.

CDK inhibitor p16 expression is up-regulated by OGF. Cell cycle progression depends on both positive and negative regulators. Expression of p16 was evaluated in synchronized SCC-1 cells after 3, 6, 9, and 12 h of OGF exposure. p16 was significantly up-regulated ($P < 0.05$) in OGF-treated cells relative to control cells only at 3 h (Fig. 3*A*). Because p16 inhibits Cdk4 by physical interaction, we examined whether the OGF-induced down-regulation of Cdk4 kinase activity was based on p16-Cdk4 complex formation. To explore this possibility, homogenates of SCC-1 cells were subjected to Cdk4 immunoprecipitation and the precipitated proteins were probed with p16 antibodies. The level of the p16-Cdk4 complex after OGF treatment was elevated at all time points compared with control and reached statistical significance ($P < 0.05$) at 9 and 12 h (Fig. 3*B*).

To show the opioid-receptor mediation of OGF, cells were treated concomitantly with the opioid antagonist naloxone and OGF. OGF-induced up-regulation of p16 expression was blocked in cells exposed to both naloxone and OGF; naloxone alone had no effect on p16 expression (Fig. 3*C*). This result showed that OGF-induced up-regulation of p16 expression was receptor mediated. p16 is known as a tumor suppressor gene, functioning as a cell cycle inhibitor by forming heterotrimeric complexes with Cdks and cyclins. Therefore, the data suggest that, under the effect of OGF, p16 protein level was up-regulated and the p16-retinoblastoma pathway was activated that, in turn, mediated the cell cycle block.

Analysis of the expression of cell cycle inhibitors p15, p18, p19, p21, and p27 revealed that OGF treatment had no significant effect on these CKIs (Fig. 4). No p57 protein was detected in SCC-1 (data not shown). Thus, OGF treatment results in the induction of only p16 in HNSCC.

siRNA directed against p16 blocked OGF inhibitory action. To test the role of p16 in OGF-induced inhibitory action on SCC-1 cell growth, siRNA knockdown experiments were used. SCC-1 cells were treated with p16 siRNA or with negative control siRNA. Western blot analysis revealed that cells transfected with p16 siRNA had significantly reduced levels of p16 protein compared with untransfected cells after 72 h (Fig. 5*A*). Growth analysis of cells transfected with p16 siRNAs and subsequently exposed to OGF for 96 h showed that p16 induction is required for the OGF inhibitory action on SCC-1 cell growth (Fig. 5*B*). SCC-1 cells transfected with the negative control siRNAs and exposed to OGF had significant reductions in growth of 24% and 40% at 72 and 96 h, respectively.

To examine the ubiquity of the integral role of p16 inhibition, two other HNSCC cell lines were examined: CAL-27 and SCC-4. In synchronized CAL-27 cells, OGF increased p16 expression at 9 h relative to controls (data not shown). Western blot analysis of protein isolated from CAL-27 cells transfected with p16 siRNA had significantly reduced p16 levels relative to control cells (data not shown). Growth curves revealed that OGF had no inhibitory effects on CAL-27 cells lacking p16 (Fig. 5*C*). In another cell line, SCC-4, OGF treatment induced p16 expression at 3 h relative to synchronized control cells (data not shown). Protein isolated from SCC-4 cells transfected with p16 siRNAs and analyzed by Western blot showed significantly reduced levels of p16 protein compared with control cells at 72 h (data not shown). Growth curves of these SCC-4 cells showed that OGF had no effect on cells lacking p16

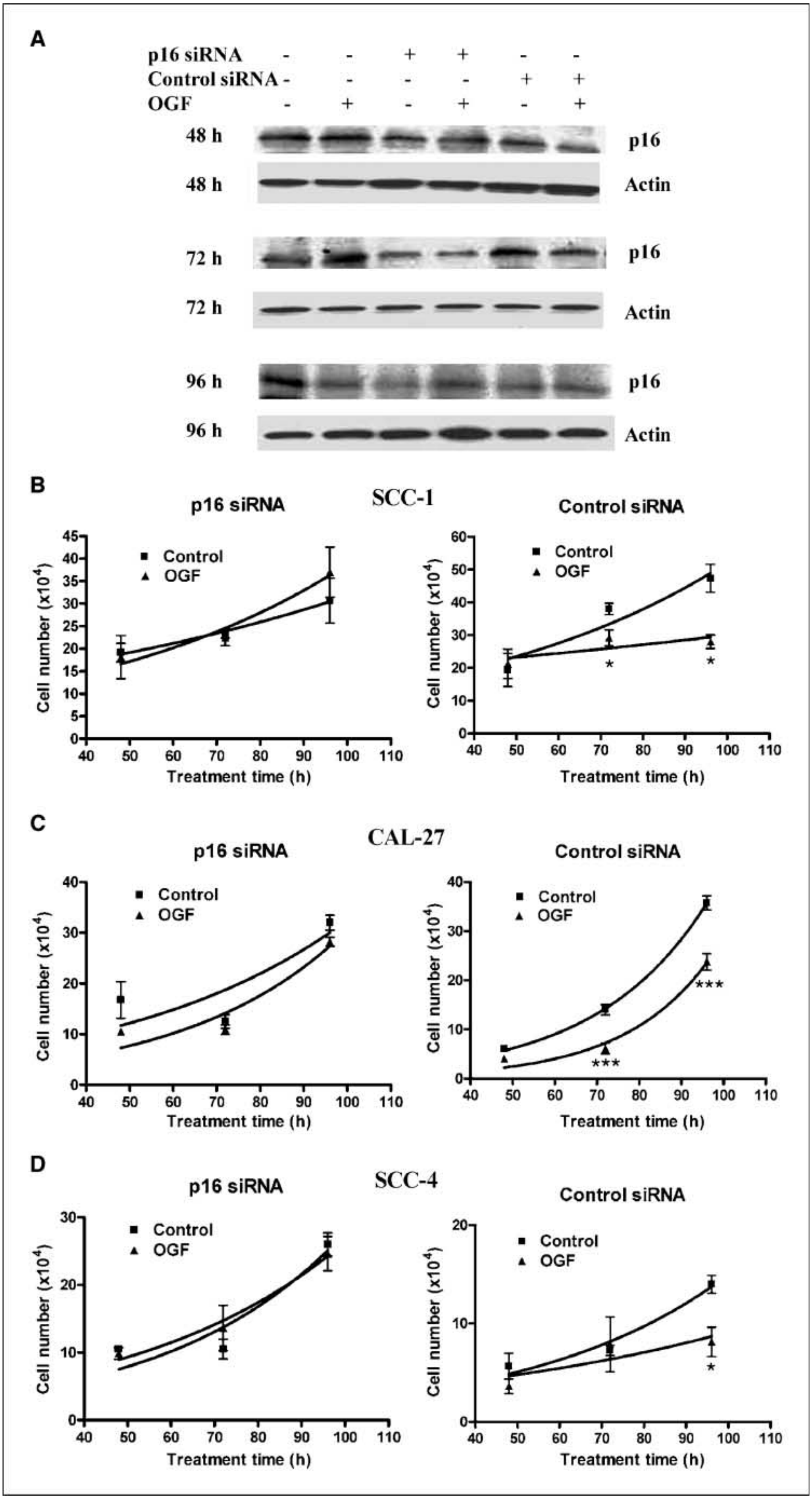

Figure 5. p16 is required for OGF-induced growth inhibition. *A,* SCC-1 cells were transfected with p16 siRNAs or control siRNAs for 48, 72, or 96 h. Total proteins were isolated and separated by SDS-PAGE and probed with antibodies specific to p16 or actin. *B-D,* growth curves for SCC-1 (*B*), CAL-27 (*C*), and SCC-4 (*D*) cells transfected with either p16 siRNA or negative control siRNA and grown in the presence or absence of 10^{-6} mol/L OGF for 96 h. Cells were harvested at 48, 72, and 96 h and counted with a hemacytometer. *Points,* means for three independent experiments; *bars,* SE. Cell numbers for OGF-treated cells were significantly reduced from control levels at $P < 0.05$ (★) and $P < 0.001$ (★★★).

expression (Fig. 5*D*) but that OGF significantly ($P < 0.05$) inhibited (a decrease of 43%) the growth of SCC-4 cells transfected with negative control siRNAs for 96 h.

Discussion

The OGF-OGFr axis has been documented by structural, pharmacologic, and biochemical evidence to be present and to function as a regulatory system for growth in HNSCC. First, OGF and OGFr have been identified in human HNSCC cell lines and surgical specimens by immunohistochemistry (4, 12–14). Second, OGFr has been characterized in human HNSCC cells and tissues by receptor binding (1, 2, 12, 13, 15) and Western blotting (12) and shown to have at least a 7-fold greater affinity for OGFr than any other natural or synthetic opioid peptide (including those specific for μ, δ, or κ classic opioid receptors; ref. 15). Third, exogenous OGF depresses the proliferation of human HNSCC cells *in vitro* (3, 4) and in xenografts (1, 2, 13), and elimination of endogenous OGF neutralizes this peptide's action on cell replication (4). However, these previous studies do not directly show that OGF, which also recognizes other classic opioid receptors (16), may also elicit naloxone-sensitive antiproliferative signaling through these receptors instead of or in addition to OGFr. The logical extension of this query is that the effects of OGF on the cell cycle may be related to OGFr and/or other opioid receptors. Using OGFr knockdown experiments, the present report now shows, for the first time, that the specific and singular receptor for OGF action on the replication of an HNSCC cell line is OGFr. Cells with silencing of OGFr are not altered by addition of OGF. Moreover, these cells with a knockdown of OGFr are not influenced by naltrexone, documenting that other opioid receptors are not involved with the effects of this general opioid receptor antagonist. Thus, the elucidation of the target of OGF in this study is directly, and solely, related to OGFr.

This study shows for the first time that the target of the negative growth regulator OGF is the cyclin-dependent kinase inhibitor p16. Using a HNSCC cell line, SCC-1, that exhibited growth inhibition after exposure to OGF and flow cytometry observations documenting that OGF impeded cells exiting G_0-G_1, we now conclude that the peptide action is related to a key regulator of the G_1-S phase transition — the tumor suppressor retinoblastoma protein. This would suggest that OGF action with regard to the cell cycle is not broad based but rather extremely specific to a pathway focused on the phosphorylation of retinoblastoma. The effects of OGF on p16 were found to be receptor mediated, as concomitant exposure to the opioid antagonist naloxone blocked the up-regulation of p16 by OGF; naloxone treatment alone had no effect on p16 levels, indicating that there was not simply a counterbalance of up-regulation and down-regulation between OGF and naloxone. Finally, confirmation that p16 was indeed the target of OGF was validated in siRNAstudies, whereas HNSCC cells exposed to p16 siRNA exhibited no change in growth after exposure to OGF. Thus, our study makes the novel finding that OGF is directed to a singular component of the cell cycle.

This investigation also shows that the action of OGF on the p16 cyclin–dependent inhibitory kinase in SCC-1 is not specific to the SCC-1 cell line but that the p16-retinoblastoma pathway is present and active in a number of other HNSCC cell lines. Thus, two other cell lines exhibiting different levels of differentiation and origin, SCC-4 and CAL-27 cell lines, showed that the p16 pathway was targeted by OGF as well. SCC-1 and SCC-4 were derived from a well-differentiated squamous cell carcinoma of the tongue in 74-year-old and 55-year-old males (4), whereas CAL-27 was derived from a poorly differentiated HNSCC of the tongue of a 56-year-old male (4). Thus, OGF seems to act on the p16 pathway in a variety of HNSCC cell lines, suggesting that this may be the primary pathway of cell cycle influence of the OGF-OGFr axis in these cancers. Whether OGF also influences p16 *in vivo* in humans is unclear and requires further study.

During the cell cycle progression, retinoblastoma is sequentially phosphorylated by different cyclin-Cdk complexes (17). Different phosphorylation sites in retinoblastoma have been shown, with the preferred site being $Ser^{807/811}$ by Cdk4-cyclin D and Thr^{821} by Cdk2 (11). Our observation that OGF down-regulated the phosphorylation of retinoblastoma on $Ser^{807/811}$ is consistent with decreased Cdk4 kinase activity. Although *in vitro* assays of Cdk4 kinase activity showed a transient increase at 3 h of OGF treatment, Cdk4 activity was decreased relative to controls at all later time points in response to OGF treatment. This reduction in Cdk4 kinase activity correlated with an increase in Cdk4-p16 complex formation in the OGF-exposed cells relative to control cultures at all time points. The transient increase in Cdk4 kinase activity at 3 h is unclear and suggests that there may be other signaling pathways affecting Cdk4 activity. We also observed that OGF had no effect on retinoblastoma Thr^{821} phosphorylation, which implies that OGF did not affect Cdk2 activity. Thus, OGF exerts its effects in these cells by inducing Cdk4-p16 complexes.

p16 has been considered as a target for potential anticancer drugs. For example, indole-3-carbinol, a naturally occurring component of Brassica vegetables, strongly stimulated the production of the p16-Cdk inhibitor and induced a block in G_1 cell cycle in LNCaP prostate carcinoma cells (18). Recently, studies showed that transfection of exogenous wild-type p16 gene induced bladder cancer cells to be arrested in G_0-G_1 phase (19). Our results with OGF and HNSCC are consistent in finding that up-regulating p16 expression has a negative effect on growth. However, in the case of HNSCC, these changes are transient and not permanent, suggesting that OGF has cytostatic, but not cytotoxic, effects. These observations support our studies showing that OGF has no effect on apoptosis (20).

The clinical ramifications of our findings merit further discussion. A review of the literature indicates that most HNSCC tumors resected in patients contain p16, hence our selection of HNSCC cell lines that were known to have p16. For example, Zhang et al. (21) have reported 10% of mutations and deletions of p16 in primary tumors and 44% in cell lines. Lydiatt et al. (22) have reported 19% of genetic alterations of p16 in HNSCC tumors and 75% in cell lines. Therefore, neoplasias with the p16 pathway would be predicted to react positively to OGF therapy. In the case of cell lines without p16, we have observed that these cells (23) do respond to OGF with regard to receptor-mediated growth inhibition. Whether they use a different cyclin-dependent inhibitory kinase pathway needs to be determined.

Acknowledgments

Received 5/23/2007; revised 7/30/2007; accepted 8/22/2007.

Grant support: Philip Morris USA, Inc. and Philip Morris International (P.J. McLaughlin).

The costs of publication of this article were defrayed in part by the payment of page charges. This article must therefore be hereby marked *advertisement* in accordance with 18 U.S.C. Section 1734 solely to indicate this fact.

We thank Renee Donahue for technical assistance with the siRNA experiments with OGFr.

References

1. McLaughlin PJ, Stack BC, Braine KM, Ruda JD, Zagon IS. Opioid growth factor inhibition of a human squamous cell carcinoma of the head and neck in nude mice: dependency on the route of administration. Int J Oncol 2004;24:227–32.
2. Jaglowski JR, Zagon IS, Stack BC, et al. Opioid growth factor enhances tumor growth inhibition and increases the survival of paclitaxel-treated mice with squamous cell carcinoma of the head and neck. Cancer Chemother Pharmacol 2005;56:97–104.
3. McLaughlin PJ, Jaglowski JR, Verderame MF, Stack BC, Leure-Dupree AE, Zagon IS. Enhanced growth inhibition of squamous cell carcinoma of the head and neck by combination therapy of paclitaxel and opioid growth factor. Int J Oncol 2005;26:809–16.
4. McLaughlin PJ, Levin RJ, Zagon IS. Regulation of human head and neck squamous cell carcinoma growth in tissue culture by opioid growth factor. Int J Oncol 1999;14:991–8.
5. Zagon IS, Wu Y, McLaughlin PJ. Opioid growth factor inhibits DNA synthesis in mouse tongue epithelium in a circadian rhythm-dependent manner. Am J Physiol 1994;267:R645–52.
6. Zagon IS, Roesener CD, Verderame MF, Ohlsson-Wilhelm BM, Levin RJ, McLaughlin PJ. Opioid growth factor regulates the cell cycle of human neoplasias. Int J Oncol 2000;17:1053–61.
7. Zagon IS, Verderame MF, McLaughlin PJ. The biology of the opioid growth factor receptor (OGFr). Brain Res Brain Res Rev 2002;38:351–76.
8. Zagon IS, Ruth TB, Leure-duPree AE, Sassani JW, McLaughlin PJ. Immunoelectron microscopic localization of the opioid growth factor receptor (OGFr) and OGF in the cornea. Brain Res 2003;967:37–47.
9. Zagon IS, Ruth TB, McLaughlin PJ. Nucleocytoplasmic distribution of opioid growth factor and its receptor in tongue epithelium. Anat Rec A Discov Mol Cell Evol Biol 2005;282:24–37.
10. Zhou HW, Lou SQ, Zhang K. Recovery of function in osteoarthritic chondrocytes induced by p16INK4a-specific siRNA *in vitro*. Rheumatology (Oxford) 2004;43:555–68.
11. Zarkowska T, Mittnacht S. Differential phosphorylation of the retinoblastoma protein by G_1/S cyclin-dependent kinases. J Biol Chem 1997;272:12738–46.
12. McLaughlin PJ, Stack BC, Levin RJ, Fedok F, Zagon IS. Defects in the OGF receptor (OGFr) in human squamous cell carcinoma of the head and neck. Cancer 2003;97:1701–10.
13. McLaughlin PJ, Levin RJ, Zagon IS. Opioid growth factor (OGF) inhibits the progression of human squamous cell carcinoma of the head and neck transplanted into nude mice. Cancer Lett 2003;199:209–17.
14. Levin RJ, Wu Y, McLaughlin PJ, Zagon IS. Expression of the opioid growth factor, [Met^5]-enkephalin, and the ζ opioid receptor in head and neck squamous cell carcinoma. Laryngoscope 1997;107:335–9.
15. McLaughlin PJ, Levin RJ, Zagon IS. The opioid growth factor receptor (OGFr) in human head and neck squamous cell carcinoma. Int J Mol Med 2000;5:191–6.
16. Leslie F. Methods used for the study of opioid receptors. Pharmacol Rev 1987;39:197–249.
17. Harbour JW, Luo RX, Dei Santi A, Postigo AA, Dean DC. Cdk phosphorylation triggers sequential intramolecular interactions that progressively block Rb functions as cells move through G_1. Cell 1999;98:859–69.
18. Zhang J, Hsu BAJ, Kinseth BAM, Bjeldanes LF, Firestone GL. Indole-3-carbinol induces a G_1 cell cycle arrest and inhibits prostate-specific antigen production in human LNCaP prostate carcinoma cells. Cancer 2003;98:2511–20.
19. Li L, Yang T, Lian X. Effects of exogenous wild-type P16 gene transfection on the expression of cell cycle-related proteins in bladder cancer cell line. Cancer Invest 2005;23:309–15.
20. Zagon IS, McLaughlin PJ. Opioids and the apoptotic pathway in human cancer cells. Neuropeptides 2003;37:79–88.
21. Zhang SY, Klein-Szanto AJ, Sauter ER, et al. Higher frequency of alterations in the p16/CDKN2 gene in squamous cell carcinoma cell lines than in primary tumors of the head and neck. Cancer Res 1994;54:5050–3.
22. Lydiatt WM, Murty VV, Davidson BJ, et al. Homozygous deletions and loss of expression of the CDKN2 gene occur frequently in head and neck squamous cell carcinoma cell lines but infrequently in primary tumors. Genes Chromosomes Cancer 1995;13:94–8.
23. Zagon IS, Smith JP, McLaughlin PJ. Human pancreatic cancer cell proliferation in tissue culture is tonically inhibited by opioid growth factor. Int J Oncol 1999;14:577–84.